Reduction in SNAP-23 Alters Microfilament Organization in Myofibrobastic Hepatic Stellate Cells

Haleigh B. Eubanks,* Elise G. Lavoie,* Jessica Goree,* Jeffrey A. Kamykowski,†
Neriman Gokden,‡ Michel Fausther,* and Jonathan A. Dranoff*

*Division of Gastroenterology and Hepatology, University of Arkansas for Medical Sciences, Little Rock, AR, USA
†Department of Physiology and Biophysics, University of Arkansas for Medical Sciences, Little Rock, AR, USA
‡Department of Pathology, University of Arkansas for Medical Sciences, Little Rock, AR, USA

Hepatic stellate cells (HSC) are critical effector cells of liver fibrosis. In the injured liver, HSC differentiate into a myofibrobastic phenotype. A critical feature distinguishing myofibroblastic from quiescent HSC is cytoskeletal reorganization. Soluble NSF attachment receptor (SNARE) proteins are important in trafficking of newly synthesized proteins to the plasma membrane for release into the extracellular environment. The goals of this project were to determine the expression of specific SNARE proteins in myofibroblastic HSC and to test whether their alteration changed the HSC phenotype in vitro and progression of liver fibrosis in vivo. We found that HSC lack the t-SNARE protein, SNAP-25, but express a homologous protein, SNAP-23. Downregulation of SNAP-23 in HSC induced reduction in polymerization and disorganization of the actin cytoskeleton associated with loss of cell movement. In contrast, reduction in SNAP-23 in mice by monogenic deletion delayed but did not prevent progression of liver fibrosis to cirrhosis. Taken together, these findings suggest that SNAP-23 is an important regular of actin dynamics in myofibroblastic HSC, but that the role of SNAP-23 in the progression of liver fibrosis in vivo is unclear.

Key words: Hepatic stellate cells (HSC); Actin cytoskeleton; SNARE protein; SNAP-23; Exocytosis

INTRODUCTION

In the setting of chronic injury, the liver undergoes progressive scar formation or fibrosis. When the progression of fibrosis is exuberant, the liver develops cirrhosis[1,2]. In the US, cirrhosis is the 12th leading cause of death and an important cause of morbidity[3].

The cellular mechanisms regulating liver fibrosis/cirrhosis have begun to be identified. Specifically, hepatic stellate cells (HSC) are known to be key effector cell of liver fibrosis[4–9]. HSC differentiate to a distinct phenotype characterized by increased proliferation, motility, contractility, and exocytosis of extracellular matrix (ECM) proteins in chronic liver injury. In the cirrhotic liver, healthy tissue is replaced by necrotic and apoptotic hepatic tissue, and prominent fibrous bands of ECM deposits bridge from central to central or portal to portal areas to form regenerative nodules[10]. Although many of the basic cellular functions of HSC have been characterized, the mechanisms that regulate cytoskeletal dynamics in these cells have not been identified.

Because HSC have the ability to secrete proteins into the extracellular space that function to impede or enhance the progression of liver fibrosis, we examined the expression of regulators of exocytosis in HSC. Exocytosis is defined as the release of vesicular cargo by fusion of the vesicular membrane with the plasma membrane, resulting in subsequent release of the contents to the outside of the cell[11]. Several SNARE (soluble NSF attachment) receptor proteins function to regulate vesicle fusion in exocytosis. There are two categories of SNARE proteins: v-SNAREs, which are incorporated into the vesicle membrane, and t-SNARES, which are located in the membranes of target compartments[12,13]. During the past two decades, the SNARE proteins imperative for secretion in neurons for neurotransmitter release at the synaptic cleft have been identified. Thus, the synapse has become the classical model or standard for studying exocytosis[14,15]. Despite this advancement, progress in defining the secretory apparatuses in other tissues of the body has lagged. The prototypic SNARE machinery required for docking

Address correspondence to Jonathan A. Dranoff, M.D., Director, Division of Gastroenterology and Hepatology University of Arkansas for Medical Sciences, 4301 W. Markham St. #567, Little Rock, AR 72205, USA. E-mail: jadranoff@uams.edu

and fusion consists of synaptobrevin (VAMP), syntaxin 1, and SNAP-25[15]. Synaptobrevin is a vesicle-associated membrane protein, and syntaxin and SNAP-25 are located on the target or plasma membrane. Synaptobrevins and syntaxins are expressed in many tissues of the body; however, SNAP-25 is confined to the neuronal system.

SNAP-23, a SNAP-25 homolog, is ubiquitously expressed and functions to facilitate vesicle membrane fusion in other tissues[16]. SNAP-23 has been shown to mediate exocytosis in mast and epithelial cells and also functions in receptor trafficking[17,18]. Because we had previously shown that HSC express SNAP-23 but not SNAP-25 (unpublished data), we investigated whether SNAP-23 regulates exocytosis and liver fibrosis. The studies here were performed both in vitro using immortalized HSC and in vitro using models of liver fibrosis in mice.

MATERIALS AND METHODS

Cell Culture and Transfection

All in vitro experiments were performed using the human HSC line hTERT[19]. Cells were cultured in Dulbecco's modified Eagle's medium (DMEM) with 10% fetal bovine serum (FBS) and 1% penicillin–streptomycin. For all experiments the media were replaced every 2 days. SNAP-23 knockdown was performed using small interfering RNA (siRNA) purchased from GE Health Care/Dharmacon (human SNAP-23, #8773). Lipofectamine 2000 (Life Technologies) was used for siRNA transfection according to the manufacturer's instructions. hTERT HSC were plated at approximately 70% confluency and allowed to adhere to the cell culture flask overnight. Cells were then transfected with SNAP-23 siRNA and allowed to incubate at 37°C for 6 h. Transfection medium was then replaced with normal media, and the cells were allowed to incubate for 72 h prior to subsequent experimental use.

Induction of Cirrhosis Using CCl_4 in SNAP-23 +/− and Wild-Type (WT) Mice

Experimental cirrhosis was induced by injection of CCl_4. Specifically, we assessed changes at the following intervals: 2 weeks to assess early fibrosis and 6 weeks to assess late fibrosis/cirrhosis.

Prior to treatment, mice were treated for 1 week with phenobarbital to upregulate P-450 enzymes to ensure consistency of fibrosis/cirrhosis in experimental animals. Then WT ($n = 10$) and SNAP-23 +/− ($n = 10$) mice were given an intraperitoneal injection of CCl_4 mixed with sterile olive oil (0.3–0.5 ml/kg, 1:1 dilution in sterile olive oil) or injected with only olive oil (control) three times a week. Subcutaneous injections of vitamin K (0.4 mg/kg) were also given to prevent bleeding. After 2 and 6 weeks, mice were sacrificed and livers were harvested. Liver tissue was analyzed for disease progression using several different biochemical approaches. To observe phenotypical expression of fibrotic factors, liver histology was analyzed by hematoxylin and eosin (H&E) staining, trichrome, and picrosirius red (PSR) staining.

Immunoblot

Total protein was extracted from livers using Tissue Protein Extraction Reagent (T-PER; Thermo Fisher Scientific). Protein was quantified using a BCA Protein Assay (Thermo Fisher Scientific) according to the manufacturer's instructions. Standard immunoblot techniques were used to detect the expression of -smooth muscle actin (-SMA). An anti-mouse monoclonal antibody to -SMA was used for immunoblotting (Sigma-Aldrich). Radioimmunoprecipitation assay (RIPA) buffer (Thermo Fisher) was used to isolate protein from hTERTs, and the BCA Protein Assay was used for protein quantification. Standard immunoblot techniques were used to detect the expression of SNAP-23, Rho, ROCK (Abcam), Cofilin, and phospho-Cofilin (Cell Signaling Technology).

Real-Time Polymerase Chain Reaction (RT-PCR)

REDExtract-N-Amp Tissue PCR Kit (Sigma-Aldrich) was used for mouse genotyping. Approximately 0.5–1 cm of mouse tail tip was incubated in a mixture of Tissue Extraction Solution (100 µl) and tissue preparation solution (25 µl) at room temperature for 10 min, making sure the tail is completely submerged in the mixture. The sample was then incubated at 95°C for 3 min. Next, 100 µl of neutralizing buffer was added to the sample and mixed by vortexing. The sample was immediately used for PCR. For the SNAP-23 +/− mouse genotyping, the PCR mixture for one sample consisted of 5 µl of Red Extract, 0.8 µl of primer mix (Table 1), 2.2 µl nuclease-free water, and 2 µl of tail snip sample. PCR conditions can be found in Table 2. SNAP-23 +/− mouse generation is described in Suh et al.[18].

Table 1. Primers for SNAP-23 +/− Mouse Genotyping (Suh et al.[30])

Primer Name	Sequence (5 -3)	Estimated PCR Product Size
genoE2 SS	TGCCCATAGGTTGTCAGACT	WT allele: 266 bp
genoNEO SS	TCACCTTAATATGCGAAGTGG	NEO+ floxed allele: 400 bp
genoE2 AS	ATGTGCTAACCATGACCTTGA	

Table 2. PCR Thermal Cycling Conditions for Genotyping

Stage	Temperature	Time
Initial denaturation	94°C	2 min
Amplification (34 cycles)	94°C	30 s
	60°C	30 s
	72°C	30 s
Final extension	72°C	10 min
Hold	4°C	

Total RNA was extracted from SNAP-23 +/− and WT mouse livers using TRIzol (Thermo Fisher Scientific) according to the manufacturer's instructions. RNA purity was assessed by A_{260}/A_{280} ratio and was quantified by fluorometry. Expression of target genes was assessed using nonquantitative RT-PCR using a Bio-Rad S1000 Thermocycler. Changes in TIMP-1, -SMA, collagen 1, and SNAP-23 mRNA copy numbers were determined by quantitative (q)RT-PCR using a Bio-Rad CFX96 Thermocycler. Target genes were normalized to beta-2-microglobulin. Primers used are summarized in Tables 3 and 4.

Isolation of Primary HSC From SNAP-23 +/− and WT Mouse Livers

Primary HSC isolation was accomplished by density gradient centrifugation using Nycodenz (Sigma-Aldrich)[20]. Briefly, SNAP-23 +/− and WT mouse livers were perfused in situ with collagenases. Afterward, the livers were extracted and teased apart into a cell suspension with forceps and subjected to multiple steps of centrifugations with protease and DNase enzymes to clean and eliminate debris. In the final steps, the cleaned cell suspensions were centrifuged over 10% Nycodenz. HSC were collected from the interface between media and Nycodenz. Isolated HSC were then plated on plastic or glass for 7 days prior to use.

Fluorescence Microscopy

Visualization of SNAP-23, -SMA, and filamentous actin was achieved using conventional fluorescence microscopy. hTERT HSC were cultured and transfected in the conditions described above. Cells were then fixed on coverslips with 4% paraformaldehyde, and rhodamine or fluorescein phalloidin was used to label all filamentous actin. Primary HSC were isolated and fixed on coverslips. Mouse anti- -SMA and rabbit anti-SNAP-23 were used to label proteins of interest. Rabbit anti- -SMA (Abcam) was used on formalin-fixed, paraffin-embedded liver sections. All fluorescent stained specimens were counterstained with 4 ,6-diamidino-2-phenylindole (DAPI) and assessed using a Zeiss AxioImager microscope.

G-Actin/F-Actin In Vivo Assay Kit

A commercial kit (Cytoskeleton Inc., Denver, CO, USA) was used to analyze the G/F-actin ratio in hTERT HSC transfected with scramble or SNAP-23 siRNA. siRNA-transfected hTERT HSC were collected and lysed in a detergent-based lysis buffer that stabilizes the G- and F-actin forms. An ultracentrifugation step pellets the F-actin and leaves the G-actin in the supernatant. Samples from each fraction were resolved using sodium dodecyl sulfate polyacrylamide gel electrophoresis (SDS-PAGE) and detected by immunoblot analysis using a rabbit anti-actin antibody provided in the kit.

Wound Healing Assay

hTERT HSC were plated and transfected with scramble or SNAP-23 siRNA. Cells were incubated for 72 h, trypsinized, and then approximately 2×10^5 hTERT HSC were plated in a 24-well plate in triplicates. Cells were allowed to grow until a monolayer formed (24 h). The cell monolayer was then scraped with a 1-ml pipette tip to create a linear "scratch." Cells were then washed twice with PBS to remove dead cells and debris. Cell migration over time was observed using a Zeiss Axiovert S100TV microscope.

Collagen Contraction Assay

The Collagen Gel Contraction Assay was adapted from published protocols using rat tail collagen 1[21]. First, cells were treated with scramble versus SNAP-23 siRNA and incubated for 72 h. A final cell population of $1 \sim 2 \times 10^5$ cell/ml was suggested. To begin, cells were washed with PBS and detached from the culture vessel with warm trypsin. Next, cells were washed with PBS to remove trypsin. Cells were then counted and adjusted to a concentration of 1.5×10^5 cells/ml. In a separate tube, 400 μl of the cell suspension was mixed with 200 μl of

Table 3. Primer Sequences for qRT-PCR

Gene	Reference Sequence Number	Company
Mouse alpha smooth muscle actin (Acta2)	NM_007392	Integrated DNA Technologies
Mouse TIMP-1	NM_011593	Integrated DNA Technologies
Mouse beta-2-microglobulin	NM_009735	Integrated DNA Technologies
Mouse collagen I (Col1a1)	Mm.277735	Thermo Fisher Scientific

All primer sequences include a FAM probe sequence.

Table 4. qRT-PCR cDNA Amplification Conditions for Determining the Expression of -SMA, Collagen 1, TIMP-1, and B2M in Mouse Livers (40 Cycles)

Stage	Temperature	Time
Polymerase activation	95°C	3 min
Amplification	95°C	10 s
Annealing and extension	57°C	30 s
	4°C	

collagen solution (3 mg/ml in 0.1% acetic acid), making the final collagen concentration 1 mg/ml. The appropriate amount of 1 M NaOH was immediately added to the cell/collagen mixture and mixed well with a pipette to avoid bubbles. Next, 500 μl of the cell/collagen mixture was pipetted into a 24-well plate, and the mixture was allowed to solidify for 20 min. Then 600 μl of culture media was gently added to the wells, and the gel was gently detached from the well using a small pipette tip. The
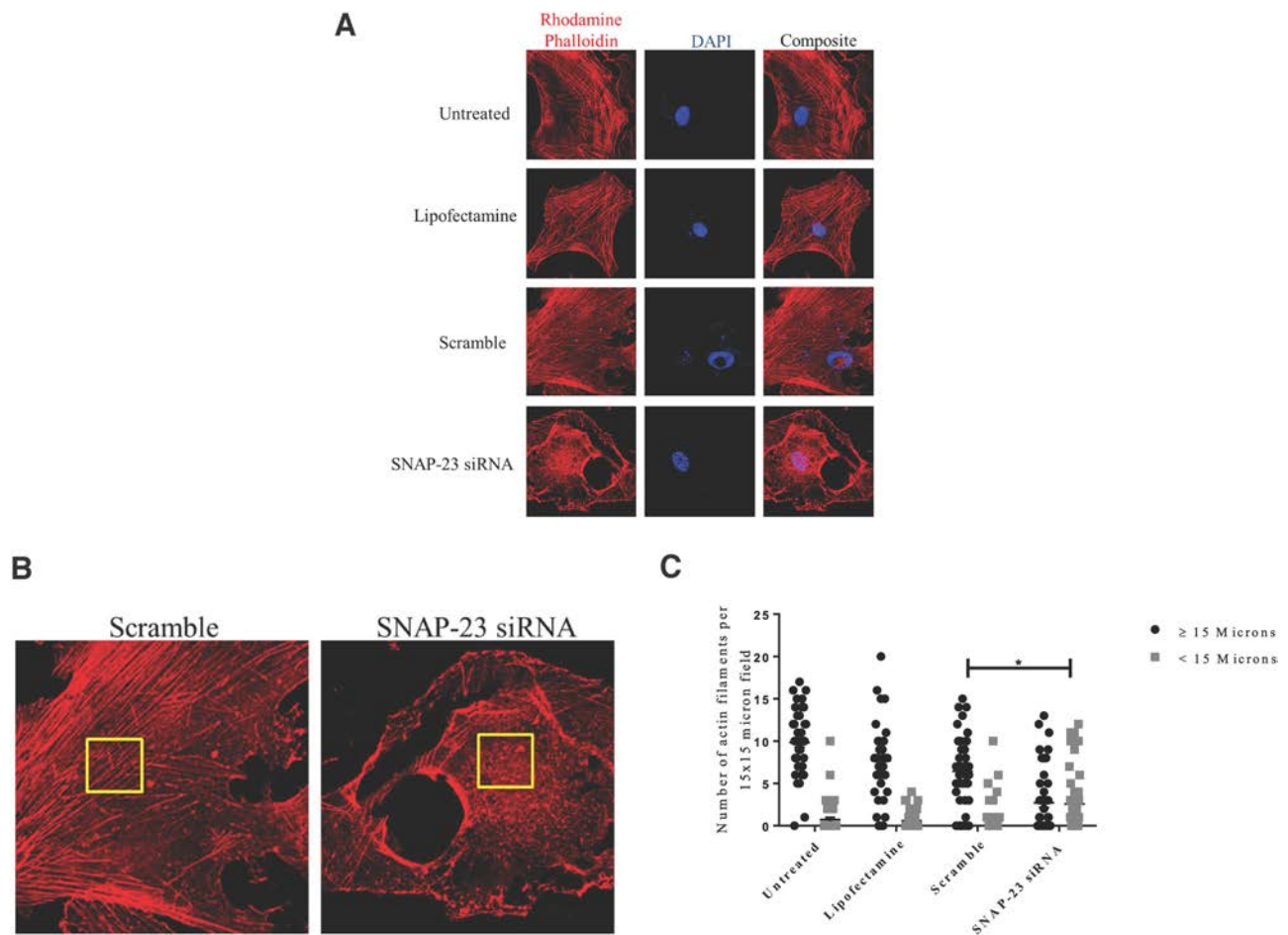
Figure 1. Reduction in SNAP-23 causes fragmentation of filamentous actin in hTERT hepatic stellate cells (HSC). (A) Change in F-actin structure. hTERT HSC were treated with scramble (control) or SNAP-23 siRNA. Rhodamine phalloidin was used to visualize total F-actin content. Nuclei were counterstained with 4 ,6-diamidino-2-phenylindole (DAPI). (B.) Quantification of F-actin morphology. ImageJ was used to create a 15×15-μm box to count the number of actin filaments of 15-μm length. Individual cells were identified by the nuclei (DAPI). At least 15 cells per condition were analyzed. Three 15×15-μm boxes were randomly placed inside each cell (45 15×15-μm boxes were analyzed for each condition). Each filament that spanned the complete box (0 μm) was counted, and also individual fragments within the box that did not span the complete box (<10 μm) were also counted. (C). Graphical representation of data in (B). Graphs are a culmination of 30 15×15-μm fields per condition *$p < 0.05$. Original magnification: 630×.

tip was carefully traced around the circumference of the gel without shearing it. Then the plate was gently swirled to make sure the gel was floating and completely dissociated from the well wall.

Quantification of Actin Junctions and Measurement of Actin Filament Length

The hTERT cell line was treated with scramble or SNAP-23 siRNA and then stained with rhodamine phalloidin to visualize total actin content. In order to better observe actin filament organization, length, and junctions, maximum intensity pixel (MIP) and Z-stack images were obtained via confocal microscopy. A 15×15-μm box was randomly placed in three areas of each cell without overlap. ImageJ was used to manually count actin filaments that were less than or greater than/equal to 10 μm in post hoc analysis.

Statistical Analysis

All data are shown as mean $\pm$ standard deviation. Paired data were assessed by parametric *t*-test, and grouped data were assessed by analysis of variance (ANOVA). Analyses were performed using GraphPad Prism 7 (GraphPad Prism Software, La Jolla, CA).

RESULTS

Reduction in SNAP-23 Alters Actin Morphology in HSC

We first tested whether reduction in SNAP-23 in hTERT cells via siRNA transfection would alter HSC phenotype. As seen in Figure 1, HSC transfected with control siRNA show filamentous actin almost exclusively in stress fibers, which is a well-established phenomenon for liver myofibroblasts[22]. In contrast, cells lacking SNAP-23 showed unexpected alterations in filamentous actin morphology. Specifically, cells lacking SNAP-23 showed actin fragmentation and cell invaginations (Fig. 1A). To quantitate the effect on actin, we analyzed 15×15-μm boxes randomly placed throughout the cell in a post hoc fashion (Fig. 1B). Aggregate data, as shown in Figure 1C, indicate that actin filaments shifted from a pattern that was almost all were >10 μm in control cells to one in which at least half of the filaments were <10 μm in SNAP-23 siRNA-transfected cells.

To verify the physiological importance of these experiments, we repeated them in primary HSC isolated from WT or SNAP-23 +/− mice. Similar to the findings in Figure 1, primary HSC from SNAP-23 +/− mice also display an anomalous α-SMA distribution pattern relative to control (Fig. 2).
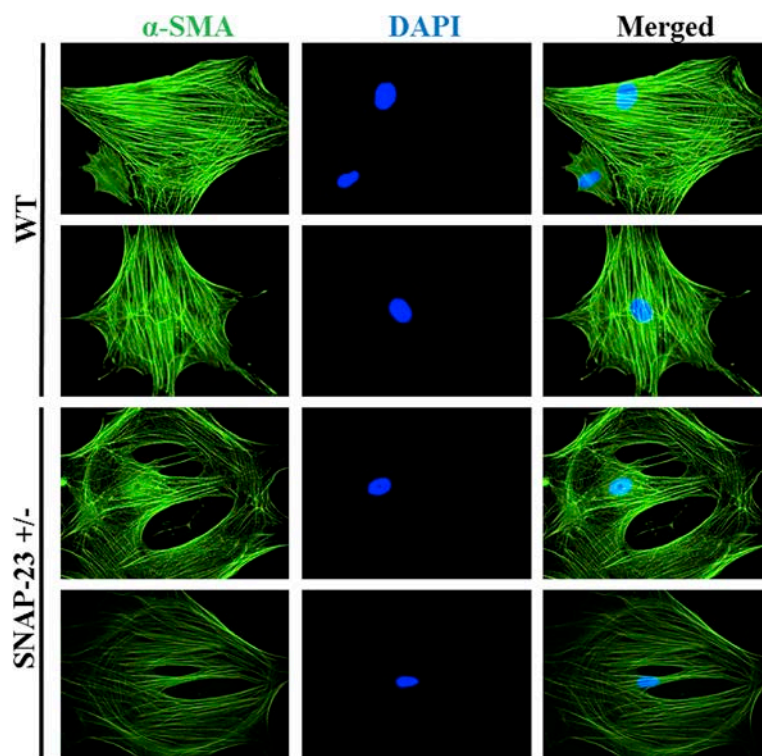

Figure 2. Primary HSC isolated from SNAP-23 +/− mice demonstrate atypical α-smooth muscle actin (α-SMA) organization. Primary HSC from wild-type (WT) and SNAP-23 +/− mice were labeled with antibodies to α-SMA (green). DAPI (blue) was used to label nuclei. As can be seen in the images, HSC from heterozygote mice show loss of classic stress fiber distribution. Original magnification: 400×.

Reduction in SNAP-23 Alters F-Actin/G-Actin Ratio in HSC

To determine whether changes in filamentous actin shown in Figures 1 and 2 were due to loss of F-actin, we performed a biochemical assay for F/G-actin ratio (Fig. 3). Reduction in SNAP-23 in hTERT resulted in a decrease in F-actin and increase in G-actin relative to control. This strongly suggests that loss of SNAP-23 alters actin polymerization dynamic equilibrium (Fig. 3).
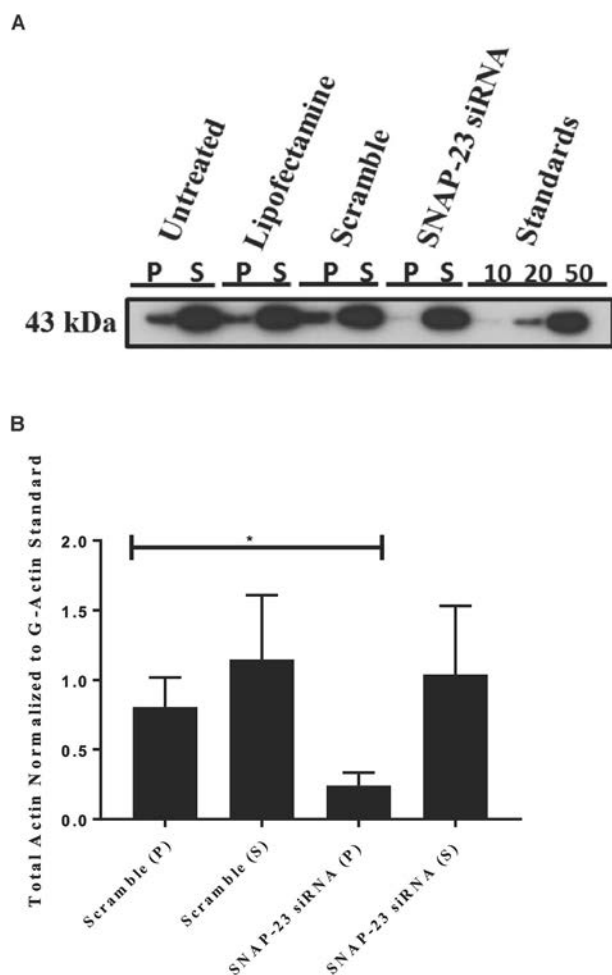

Figure 3. Knockdown of SNAP-23 reduces F-actin polymerization in hTERT HSC. (A) hTERT HSC were treated with scramble (control) or SNAP-23 siRNA. A commercial G/F-actin assay was used to assess the changes in globular and filamentous actin in the supernatant and pellet fractions, respectively. As can be seen via Western blot analysis, a reduction in SNAP-23 significantly decreases the amount of filamentous actin in the pellet. Experimental bands were compared to actin standards of 10, 20, and 50 ng. (B) Quantification of data shown in (A). $n = 3$ for all conditions. *$p < 0.05$ scramble versus SNAP-23 siRNA. The abbreviations P and S mean pellet and supernatant.

Reduction in SNAP-23 Alters HSC Migratory Function

Activated HSC are highly mobile and contractile[23]. To determine whether the change noted in filamentous actin structure and total content was associated with functional outcomes, we investigated whether a reduction in SNAP-23 in hTERT HSC regulated mobility and contraction via a wound healing assay (Fig. 4). SNAP-23 siRNA-treated hTERT HSC were unable to migrate into the wound, whereas control cells did so effectively. Figure 5 shows a collagen gel contraction assay that measures hTERT contractility. Unlike the data noted above, reduction in SNAP-23 showed no change in contractility relative to control. Taken together, these data show that SNAP-23, likely due to its effect on filamentous actin, regulates HSC migration but not contractility.

SNAP-23 Does Not Regulate Filamentous Actin via Kinase Pathways Investigated

Rho kinase pathway activation is an important regulator of actin organization in a variety of cell types, so we investigated whether knockdown of SNAP-23 in hTERT HSC would alter the expression of downstream effector proteins of Rho/ROCK. As seen in Figure 6A, there is no apparent change in ROCK1 protein expression.

F-actin is disassembled by cofilin, but not in its phosphorylated form, so loss of cofilin (or increase in phospho-cofilin) may be associated with F-actin stabilization. Figure 6B and C shows that SNAP-23-deficient hTERT cells exhibit potent downregulation of cofilin and modest downregulation of phospho-cofilin relative to control. This suggests that SNAP-23 may work in part via cofilin/phosphor-cofilin intermediates, although the mechanism by which this occurs is not clear.

Lastly, we tried to determine whether SNAP-23 and F-actin interacted via super-resolution microscopy colocalization experiments (Fig. 7). After analysis of >20 sections, we found that there is no overlap of the fluorescent signals from anti-SNAP-23 and fluorescein isothiocyanate (FITC)-phalloidin. This is emphasized by having a Pearson's coefficient of 0, showing that there is no colocalization of the fluophores. Thus, SNAP-23 and F-actin are found in distinct subcellular compartments to the limits of what can be detected using super-resolution microscopy approaches.

SNAP-23 +/− Mice Develop Delayed Experimental Liver Fibrosis

We conducted a series of experiments to determine the importance of SNAP-23 in the pathogenesis of liver fibrosis in vivo. After 2 weeks of CCl_4 exposure, at which
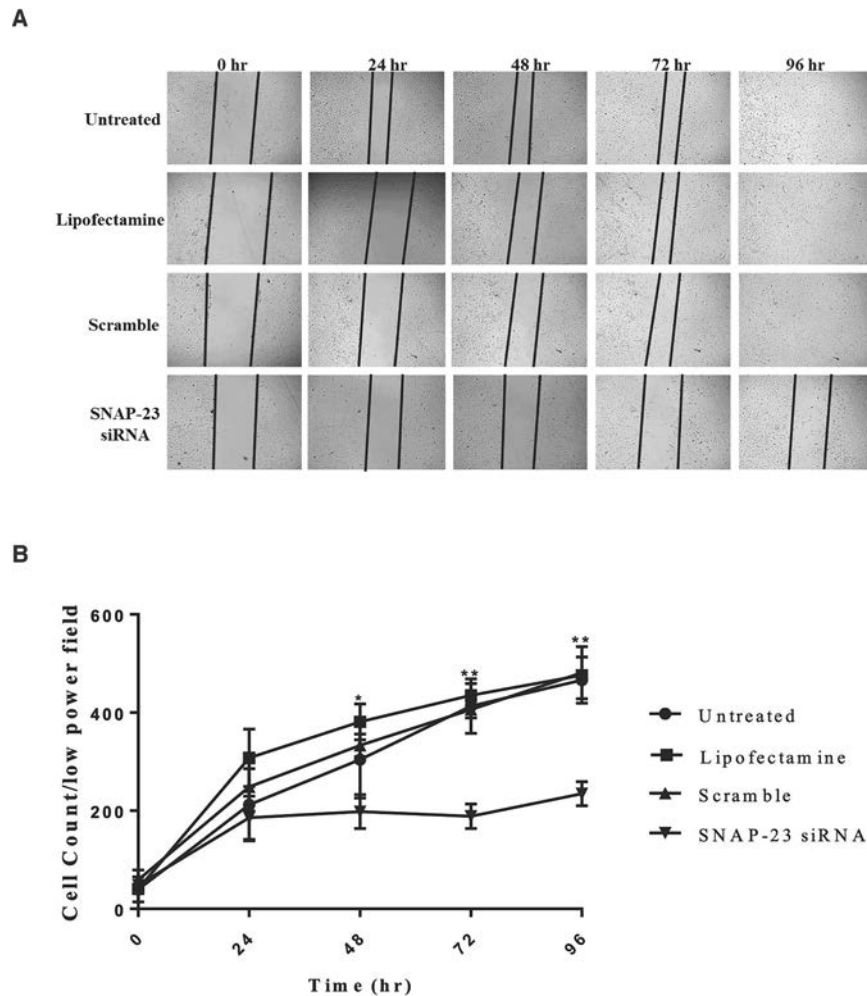
Figure 4. Reduction in SNAP-23 in hTERTs impairs cell migration. (A) Cells were transfected with scramble or SNAP-23 siRNA. An initial scratch of ~0.9 mm was placed, and cells were photographed over time. Compared to controls, cells deficient in SNAP-23 showed impaired wound closure and decreased number of cells migrating into the wound. Images shown at 2.5× magnification. (B) Quantification of data in (A). Upper graph shows cell number within the scratch. $n = 4$ for all experiments. $*p < 0.05$.

time mice typically show early to moderate fibrosis, SNAP-23 +/− mice showed decreased fibrotic stage (Fig. 8). However, after 6 weeks of CCl_4 exposure, at which time mice typically show advanced fibrosis/cirrhosis, there was no statistical difference in fibrotic stage between WT and SNAP-23 +/− (Fig. 9).

To investigate whether other parameters of liver fibrosis were altered at the 6-week time point, we determined relative transcript levels of profibrotic genes, -SMA, collagen, and TIMP-1 were changed during experimental fibrosis. As seen in Figure 10, TIMP-1 and collagen mRNA were unchanged between SNAP-23 +/− mice and controls; however, there was a significant decrease in -SMA mRNA (Fig. 10B). We then investigated whether this was associated with a change in -SMA at the protein level. As assessed by Western

blot and fluorescence microscopy, Figure 11 shows that SNAP-23 +/− CCl_4-treated mice develop less -SMA at the protein level compared to WT CCl_4-treated mice. Taken together, these data show that SNAP-23 reduction is associated with both delayed liver fibrosis and a downregulation of -SMA; however, SNAP-23 +/− mice were still able to develop cirrhosis after a sufficient exposure to CCl_4.

DISCUSSION

At present, there is a disconnect between advances in the pathophysiology of cirrhosis and clinical therapies to prevent or treat cirrhosis[24]. HSC are key effector cells of liver fibrosis and have become leading pharmaceutical targets; however, understanding of subcellular structures in HSC has been insufficiently
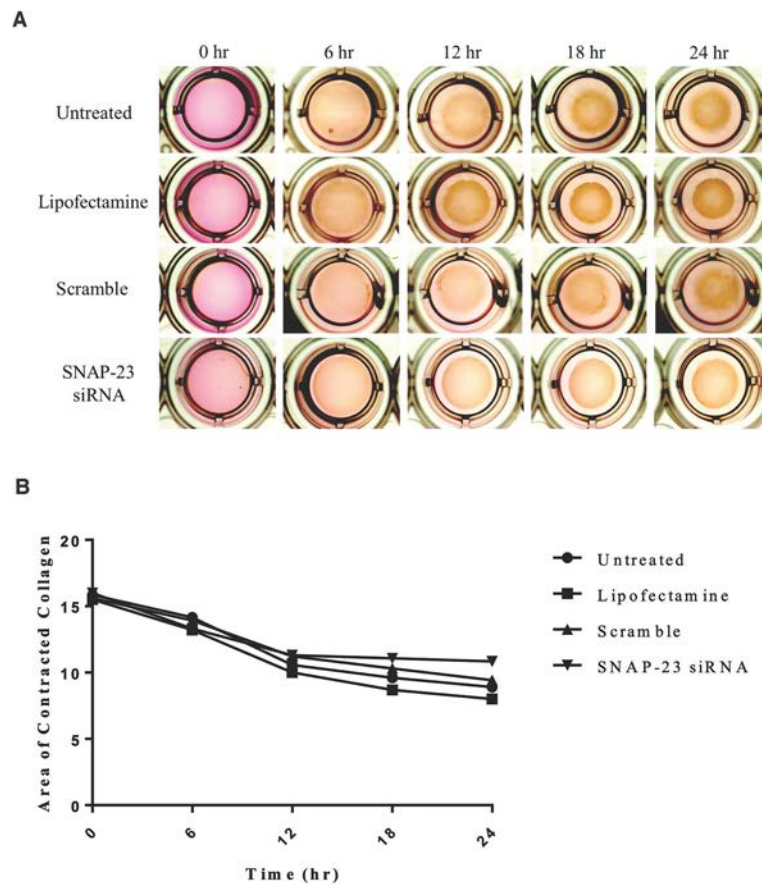
Figure 5. SNAP-23 downregulation does not alter collagen gel contraction. (A) hTERT HSC under various conditions were mixed in a collagen suspension and plated. Contraction was visualized over time by microscopy. (B) Quantification of data in (A). ImageJ was used to measure the area of each gel. No change in gel area was seen in any condition ($n = 3$ for all experiments). Original magnification: 1.5×.

explored. Our studies began with the analysis of the key docking and fusion SNARE protein, SNAP-23. We discovered that knockdown of SNAP-23 in hTERT HSC disrupted actin stress fiber organization. We also detected a similar actin distribution in primary cells isolated from SNAP-23 +/− mice. This compelled us to further investigate the importance of SNAP-23 in HSC cytoskeleton organization. SNAP-23 has been shown to be critical for cell survival and functions in several biological processes such as exocytosis and protein/receptor trafficking[18,25], but is less well defined in microfilament organization.

To our surprise, we found an unconventional role of SNAP-23 in HSC cytoskeletal organization. A brief summary of the experimental findings is as follows: (1) reduction in SNAP-23 in hTERT HSC disrupts actin morphology, (2) migratory properties, but not contractile properties, are compromised in hTERT HSC treated with SNAP-23 siRNA, (3) changes in the HSC actin

morphology are possibly due to alterations in cofilin dynamics, (4) SNAP-23 and actin do not colocalize, ruling out the possibility of direct physical interaction, (5) SNAP-23 +/− mice expressed less -SMA at the transcriptional and protein level compared to WT litter mates after CCl$_4$-cirrhosis, and (6) SNAP-23 +/− mice developed fibrosis more slowly than WT litter mates. Target SNARE proteins, SNAP-25 and SNAP-23, have been shown to interact with multiple cytoskeletal proteins in various cell types[26,27]. Taken together, these studies suggest that SNAP-23 strongly regulates actin dynamics, although the mechanisms by which this occurs are not fully known.

Actin stress fiber organization is essential for HSC activation[28]. The actomyosin system functions in cell shape/integrity, division/replication, adhesion, and chemotaxis[29]. Moreover, Roche and colleagues have shown that SNAP-23 is critical for cell growth and survival, so the concept that a reduction in SNAP-23
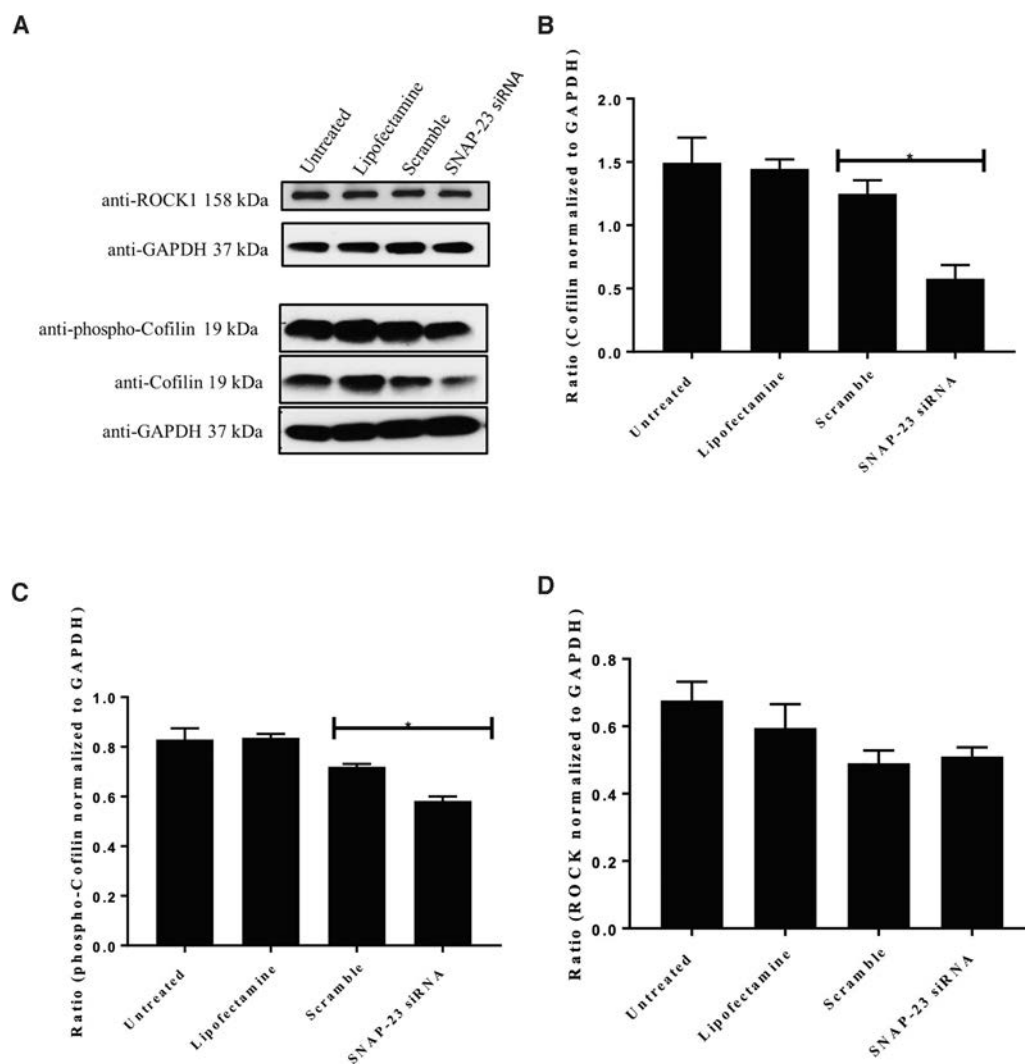
Figure 6. Downregulation of SNAP-23 had different effects on expression of ROCK1, p-cofilin, and cofilin. (A) Immunoblot of hTERT HSC transfected with scramble or SNAP-23 siRNA. Changes in the expression of ROCK, cofilin, and phospho-cofilin were assessed via immunoblot with glyceraldehyde 3-phosphate dehydrogenase (GAPDH) as a loading control. (B) Quantification of data in (A). Total and p-cofilin were significantly downregulated, although downregulation of p-cofilin was meager (B, C). No change in ROCK1 was noted (D). $n = 3$ for all conditions. $*p < 0.05$.

dismantles the HSC microfilament infrastructure in SNAP-23 siRNA-treated hTERT HSC and SNAP-23 +/− primary cells is both innovative and plausible[30]. The HSC actin stress fiber organization and functions of migration and contraction have been explored previously, albeit in different contexts. A similar pattern of actin filament disorganization has been noted in several other HSC models using inhibitors that interrupt signaling cascades that control proper actin polymerization and HSC migratory/contractile function[31–33]. Several researchers have investigated changes in the Rho/ROCK pathway, since this pathway can directly regulate actin filament organization/stabilization. Although we cannot

currently make any conclusions as to what pathway is orchestrating these outcomes, an alternative would be to investigate other downstream pathways, such as the p38 MAPK pathway and SMAD signaling pathway, also reported to be key mediators of actin organization. Another logical proposal would be to look at the ratio of profilin (actin assembly) to cofilin (actin disassembly) within HSC lacking SNAP-23. This would give insight to the polymerization and disassembly process of actin filaments resulting in fragmented actin. Also, HSC migration and contraction have been shown to be impaired in HSC with disrupted actin filaments. Our data show that migration, but not contraction, was impaired
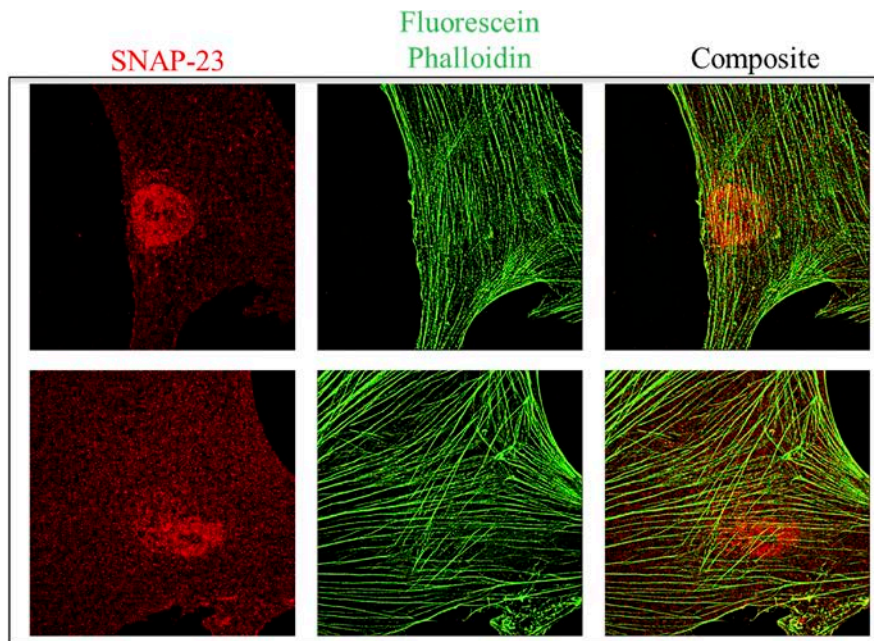
Figure 7. SNAP-23 does not colocalize with filamentous actin in hTERT HSC. Untreated hTERT HSC were stained with anti-SNAP-23 using a fluorescent secondary antibody and colabeled with fluorescein-phalloidin to visualize total filamentous actin. Super-resolution microscopy was used to assess the localization of SNAP-23 and F-actin (630×). As seen above, there is no overlap of the fluorescent signals. Pearson's coefficient (R) = 0. Experiment is representative of n = 10 slides.

in SNAP-23 +/− cells. We speculate that an axis independent of SNAP-23 is being used for cell contraction.

The finding that SNAP-23 +/− acquired fibrosis/cirrhosis at a later time point gives us insight on multiple aspects of fibrosis pathogenesis. Of note, we chose the SNAP-23 +/− mouse line because its reduction in SNAP-23 has been shown to be commensurate with protein function. Of note, complete deletion of the SNAP-23 gene is embryonically lethal. After our in vivo studies, we can assert that SNAP-23 mice do have a delayed fibrogenic response to CCl_4. However, the mechanism by which the SNAP-23 +/− mouse has delayed liver fibrosis is unknown. One caveat to inferences gained from the in vitro siRNA experiments is that the effects of the siRNA are likely more potent than the effect of single gene deletion. An alternative in vivo model would be to use a SNAP-23 floxed mouse under an HSC-specific promoter to conditionally delete SNAP-23 in activated HSC[34,35]. Roche and colleagues used a CD19-Cre-expressing mouse to delete SNAP-23 in B lymphocytes and T lymphocytes, which prevents the development of T lymphocytes. Interestingly, cells lacking SNAP-23 were highly apoptotic in this model, suggesting its potential utility to be adapted for studies of liver fibrosis.

The limitations of this study are noteworthy. It is apparent that we did not mirror every hTERT HSC experiment in primary HSC, although the experiments are analogs. Hopefully, advances in handling of primary mouse liver cell cultures will allow such experiments to be performed in the future. Interestingly, one disadvantage that we noted experimentally is that HSC isolation yields from SNAP-23 +/− mice were lower than those from WT mice. This may be due to alterations in cell attachment or even cell proliferation.

Disruption of filamentous actin causes HSC to decrease expression of -SMA and collagen[28]. Cells have also been reported to divert to the apoptosis pathway if there is dysregulation in actin filament organization and stabilization. Hence, this has become an attractive pharmaceutical target for decreasing the number of activated HSC in liver fibrosis.

In summary, these finding suggest that the SNARE protein SNAP-23 directly or indirectly plays a role in microfilament organization in HSC. Changes in SNAP-23 had important physiological effects in vitro and in vivo. Drug design may take advantage of proteins such as SNAP-23 that regulate the actin cytoskeleton, since this appears to be important in the pathophysiology of liver fibrosis/cirrhosis.
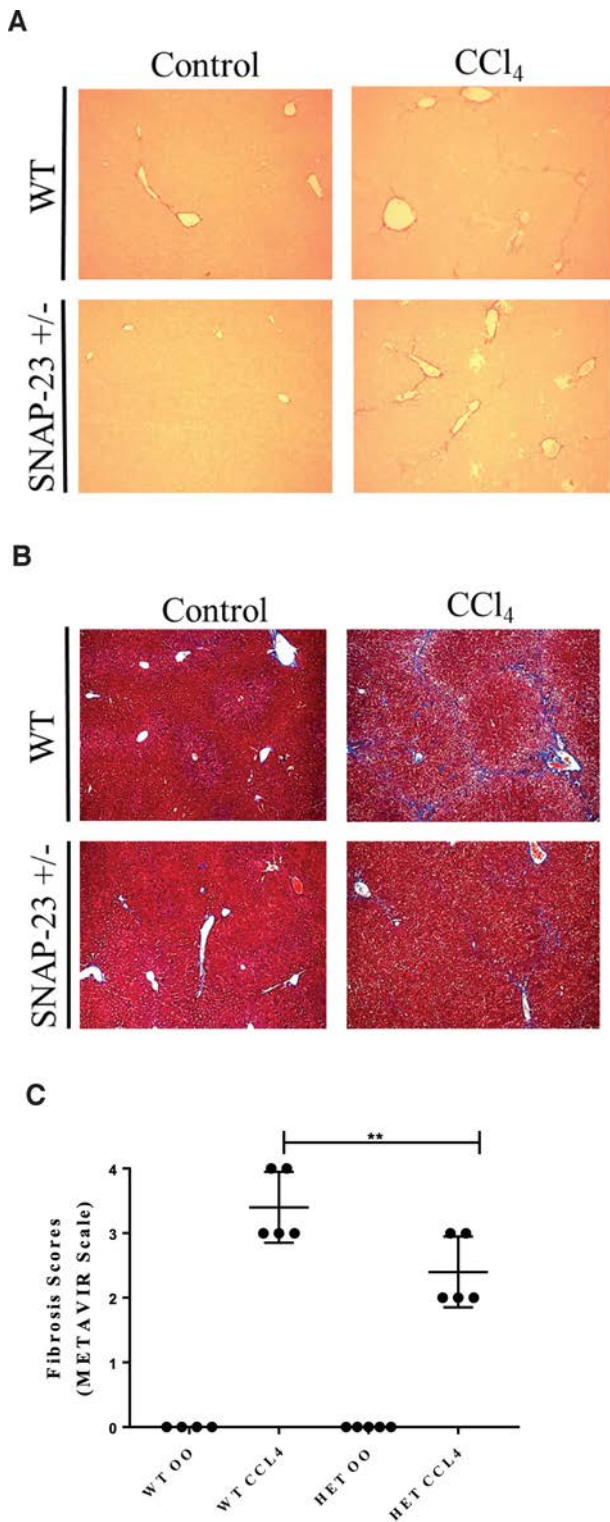
Figure 8. SNAP-23 +/− mice develop less fibrosis compared to WT mice after 2 weeks of CCl_4. (A) Picosirius red. (B) Trichrome. (C) Liver fibrosis staging. WT CCl_4 versus SNAP-23 +/− CCl_4. $n = 5$ for all conditions. **$p < 0.01$. Original magnification: 100×.
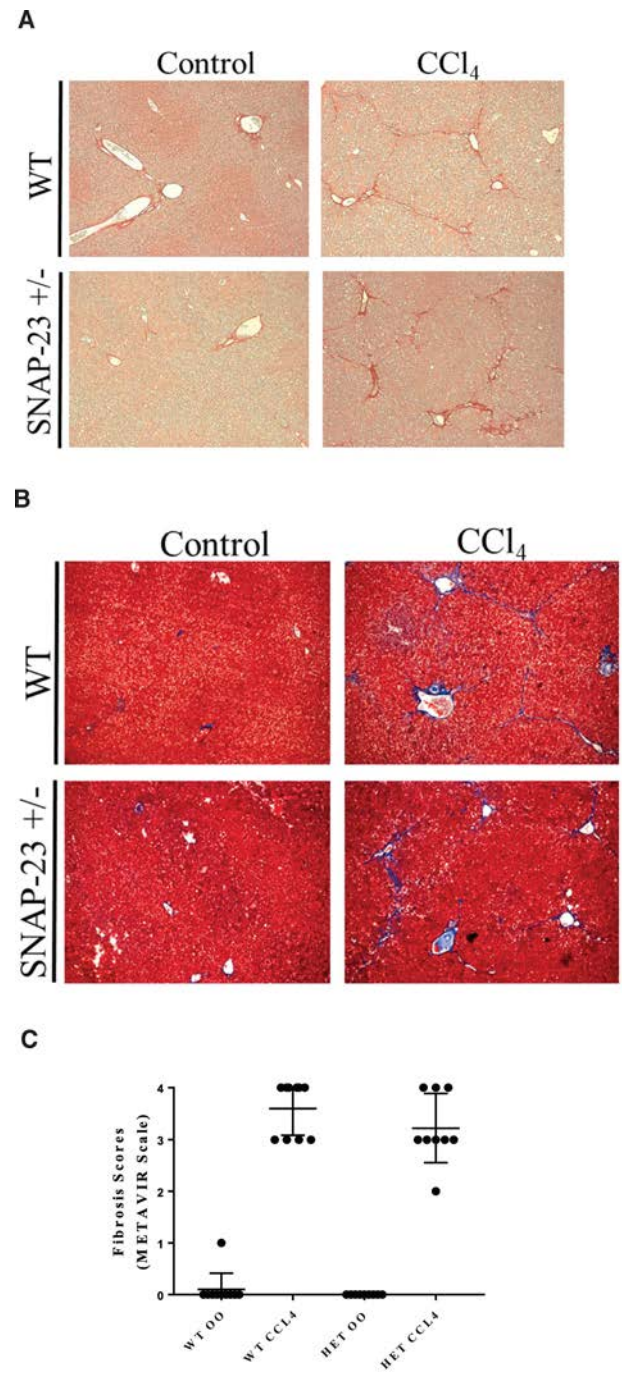

Figure 9. SNAP-23 +/− mice develop the same amount of fibrosis as WT mice after 6 weeks of CCl_4. (A) Picosirius red. (B) Trichrome. (C) Liver fibrosis staging. $n = 10$ for all conditions; WT CCl_4 versus HET CCl_4. $p = $ ns. Original magnification: 100×.
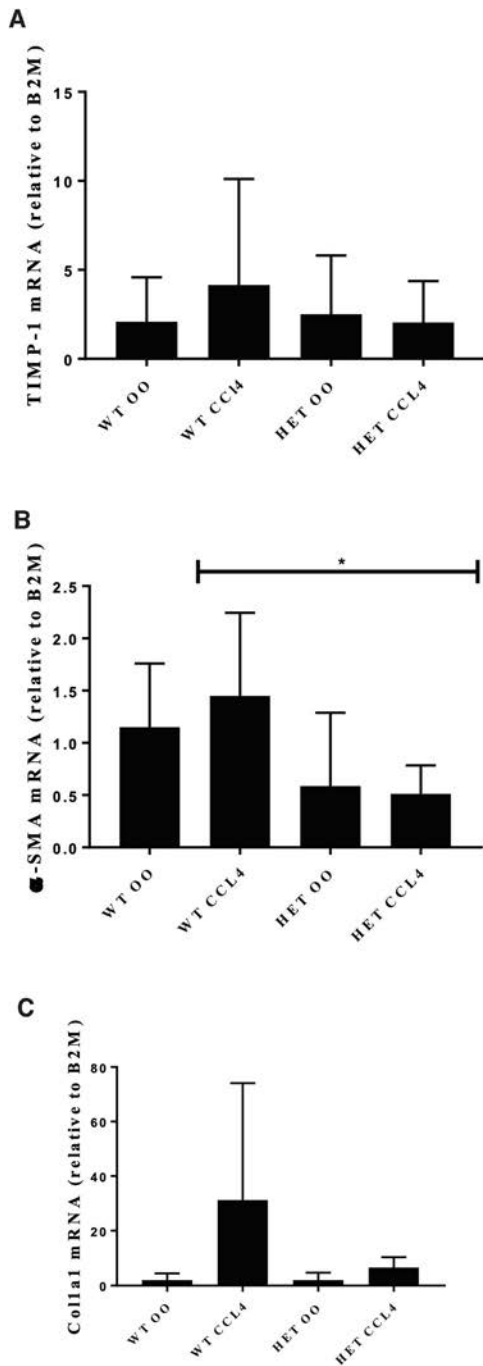
A

B

C

Figure 10. Fibrosis-associated genes are altered in SNAP-23 +/− CCl_4 mice at 6 weeks. (A) TIMP-1. No change detected in any condition. $p = 0.3475$. (B) -SMA. *$p < 0.05$ WT CCl_4 versus HET CCl_4. (C) Col1a1. $p = 0.124$ WT CCl_4 versus HET CCl_4. $n = 10$ for all conditions.
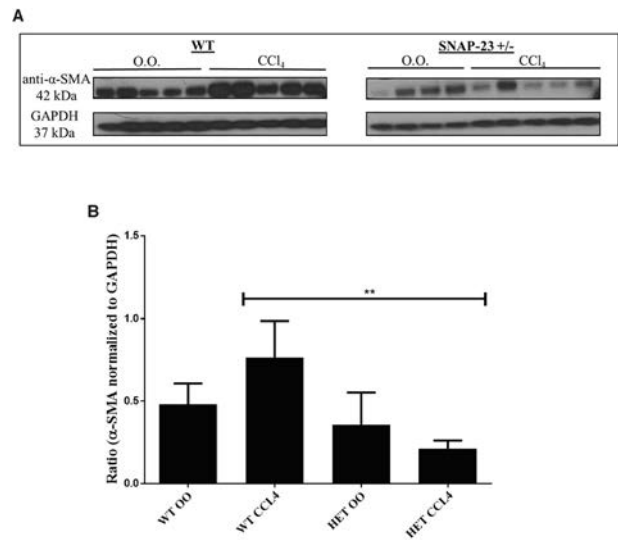
A

B

Figure 11. SNAP-23 +/− mice treated with CCl_4 express less -SMA compared to WT CCl_4-treated mice. (A) WT and SNAP-23 +/− mice were treated with CCl_4 for 6 weeks. Assessed by immunoblot, SNAP-23 +/− express less -SMA at the protein level. (B) Quantification of (A). Graph represents quantification of the -SMA blot normalized to GAPDH. WT CCl_4 versus SNAP-23 CCl_4. **$p < 0.005$. Images representative of $n = 10$. Original magnification: 100×.

REFERENCES

1. Asrani SK, Kamath PS. Natural history of cirrhosis. Curr Gastroenterol Rep. 2013;15(2):308.
2. Tsochatzis EA, Bosch J, Burroughs AK. Liver cirrhosis. Lancet 2014;383(9930):1749–61.
3. Starr SP, Raines D. Cirrhosis: Diagnosis, management, and prevention. Am Fam Physician 2011;84(12):1353–9.
4. Burt AD. Pathobiology of hepatic stellate cells. J Gastroenterol. 1999;34(3):299–304.
5. Friedman SL. The virtuosity of hepatic stellate cells. Gastroenterology 1999;117(5):1244–6.
6. Friedman SL. Mechanisms of hepatic fibrogenesis. Gastroenterology 2008;134(6):1655–69.
7. Hautekeete ML, Geerts A. The hepatic stellate (Ito) cell: Its role in human liver disease. Virchows Arch. 1997;430(3):195–207.
8. Mathew J, Geerts A, Burt AD. Pathobiology of hepatic stellate cells. Hepatogastroenterology 1996;43(7):72–91.
9. Sato M, Suzuki S, Senoo H. Hepatic stellate cells: Unique characteristics in cell biology and phenotype. Cell Struct Funct. 2003;28(2):105–12.
10. Bataller R, Brenner DA. Liver fibrosis. J Clin Invest. 2005;115(2):209–18.

11. Ramakrishnan NA, Drescher MJ, Drescher DG. The SNARE complex in neuronal and sensory cells. Mol Cell Neurosci. 2012;50(1):58–69.

12. Chen YA, Scheller RH. SNARE-mediated membrane fusion. Nat Rev Mol Cell Biol. 2001;2(2):98–106.

13. Salaun C, James DJ, Greaves J, Chamberlain LH. Plasma membrane targeting of exocytic SNARE proteins. Biochim Biophys Acta 2004;1693(2):81–9.

14. Jahn R, Fasshauer D. Molecular machines governing exocytosis of synaptic vesicles. Nature 2012;490(7419):201–7.

15. Rizo J, Rosenmund C. Synaptic vesicle fusion. Nat Struct Mol Biol. 2008;15(7):665–74.

16. Ravichandran V, Chawla A, Roche PA. Identification of a novel syntaxin- and synaptobrevin/VAMP-binding protein, SNAP-23, expressed in non-neuronal tissues. J Biol Chem. 1996;271(23):13300–3.

17. Lemons PP, Chen D, Whiteheart SW. Molecular mechanisms of platelet exocytosis: Requirements for alpha-granule release. Biochem Biophys Res Commun. 2000;267(3):875–80.

18. Suh YH, Terashima A, Petralia RS, Wenthold RJ, Isaac JT, Roche KW, Roche PA. A neuronal role for SNAP-23 in postsynaptic glutamate receptor trafficking. Nat Neurosci. 2010;13(3):338–43.

19. Schnabl B, Choi YH, Olsen JC, Hagedorn CH, Brenner DA. Immortal activated human hepatic stellate cells generated by ectopic telomerase expression. Lab Invest. 2002;82(3):323–33.

20. Mederacke I, Dapito DH, Affo S, Uchinami H, Schwabe RF. High-yield and high-purity isolation of hepatic stellate cells from normal and fibrotic mouse livers. Nat Protoc. 2015;10(2):305–15.

21. Su L, Huang L, Xu Y, Zhang C, Song Z. Quantitative analysis of collagen produced by rabbit keratocytes using second harmonic generation microscopy. Curr Eye Res. 2017;42(2):195–200.

22. Friedman SL. Hepatic stellate cells: Protean, multifunctional, and enigmatic cells of the liver. Physiol Rev. 2008;88(1):125–72.

23. Fausther M, Lavoie EG, Dranoff JA. Contribution of myofibroblasts of different origins to liver fibrosis. Curr Pathobiol Rep. 2013;1(3):225–230.

24. Torok NJ, Dranoff JA, Schuppan D, Friedman SL. Strategies and endpoints of antifibrotic drug trials: Summary and recommendations from the AASLD Emerging Trends Conference, Chicago, June 2014. Hepatology 2015;62(2):627–34.

25. Mendez M, Gaisano HY. Role of the SNARE protein SNAP23 on cAMP-stimulated renin release in mouse juxtaglomerular cells. Am J Physiol Renal Physiol. 2013;304(5):F498–504.

26. Sorensen JB, Nagy G, Varoqueaux F, Nehring RB, Brose N, Wilson MC, Neher E. Differential control of the releasable vesicle pools by SNAP-25 splice variants and SNAP-23. Cell 2003;114(1):75–86.

27. Vogel K, Roche PA. SNAP-23 and SNAP-25 are palmitoylated in vivo. Biochem Biophys Res Commun. 1999;258(2):407–10.

28. Cui X, Zhang X, Yin Q, Meng A, Su S, Jing X, Li H, Guan X, Li X, Liu S, et al. F-actin cytoskeleton reorganization is associated with hepatic stellate cell activation. Mol Med Rep. 2014;9(5):1641–7.

29. Ohashi K, Nagata K, Maekawa M, Ishizaki T, Narumiya S, Mizuno K. Rho-associated kinase ROCK activates LIM-kinase 1 by phosphorylation at threonine 508 within the activation loop. J Biol Chem. 2000;275(5):3577–82.

30. Suh YH, Yoshimoto-Furusawa A, Weih KA, Tessarollo L, Roche KW, Mackem S, Roche PA. Deletion of SNAP-23 results in pre-implantation embryonic lethality in mice. PLoS One 2011;6(3):e18444.

31. Kawada N, Seki S, Kuroki T, Kaneda K. ROCK inhibitor Y-27632 attenuates stellate cell contraction and portal pressure increase induced by endothelin-1. Biochem Biophys Res Commun. 1999;266(2):296–300.

32. Sohail MA, Hashmi AZ, Hakim W, Watanabe A, Zipprich A, Groszmann RJ, Dranoff JA, Torok NJ, Mehal WZ. Adenosine induces loss of actin stress fibers and inhibits contraction in hepatic stellate cells via Rho inhibition. Hepatology 2009;49(1):185–94.

33. Tada S, Iwamoto H, Nakamuta M, Sugimoto R, Enjoji M, Nakashima Y, Nawata H. A selective ROCK inhibitor, Y27632, prevents dimethylnitrosamine-induced hepatic fibrosis in rats. J Hepatol. 2001;34(4):529–36.

34. Greenhalgh SN, Conroy KP, Henderson NC. Cre-ativity in the liver: Transgenic approaches to targeting hepatic nonparenchymal cells. Hepatology 2015;61(6):2091–9.

35. Kaul S, Mittal SK, Feigenbaum L, Kruhlak MJ, Roche PA. Expression of the SNARE protein SNAP-23 is essential for cell survival. PLoS One 2015;10(2):e0118311.